



Identifying passivated dynamic force microscopy tips on H:Si(100)

Peter Sharp, Sam Jarvis, Richard Woolley, Adam Sweetman, Lev Kantorovich, Chris Pakes, and Philip Moriarty

Citation: [Applied Physics Letters](#) **100**, 233120 (2012); doi: 10.1063/1.4726086

View online: <http://dx.doi.org/10.1063/1.4726086>

View Table of Contents: <http://scitation.aip.org/content/aip/journal/apl/100/23?ver=pdfcov>

Published by the [AIP Publishing](#)



Re-register for Table of Content Alerts

Create a profile.



Sign up today!



Identifying passivated dynamic force microscopy tips on H:Si(100)

Peter Sharp,¹ Sam Jarvis,² Richard Woolley,¹ Adam Sweetman,¹ Lev Kantorovich,² Chris Pakes,³ and Philip Moriarty^{1,a)}

¹*School of Physics and Astronomy, The University of Nottingham, Nottingham NG7 2RD, United Kingdom*

²*Department of Physics, King's College London, The Strand, London WC2R 2LS, United Kingdom*

³*Department of Physics, La Trobe University, Victoria 3086, Australia*

(Received 21 February 2012; accepted 19 May 2012; published online 8 June 2012)

The chemical reactivity of the tip plays a central role in image formation in dynamic force microscopy, but in very many cases the state of the probe is a key experimental unknown. We show here that an H-terminated and thus chemically unreactive tip can be readily identified via characteristic imaging and spectroscopic ($F(z)$) signatures, including, in particular, contrast inversion, on hydrogen-passivated Si(100). We determine the tip apex termination by comparing site-specific difference force curves with the results of density functional theory, providing a clear protocol for the identification of chemically unreactive tips on silicon surfaces. © 2012 American Institute of Physics. [<http://dx.doi.org/10.1063/1.4726086>]

The ability to characterize and control the apex of the tip of a scanning probe microscope (SPM) plays a crucial role in ultrahigh resolution microscopy,^{1–7} atomic and molecular manipulation,^{8–10} and spectroscopic probing of interatomic and intermolecular interactions.^{8,11,12} Of particular interest in many scanning probe experiments is the passivation of a tip, i.e., the termination of dangling bonds at its apex via hydrogen or another species subsequently giving rise to a very weak chemical interaction with the underlying surface. This type of passivated tip has been exploited by a number of groups including Gross *et al.*,² where they used a CO molecule to facilitate extremely high resolution imaging of pentacene, and by Temirov *et al.*⁵ who found that hydrogen trapped in the tip-sample junction provided significant increases in resolution during scanning tunnelling microscope (STM) imaging. In both of these cases, the imaging mechanism arises fundamentally from interactions in the Pauli exclusion regime of the tip-sample interaction potential.

To date, however, the influence of passivation of a tip on scanning probe imaging of a semiconductor has not been examined experimentally nor elucidated. Although the H:Si(100) surface has been investigated in considerable detail using STM (Refs. 13–15) and has been the focus of a series of elegant atomic manipulation demonstrations involving tip-induced hydrogen desorption and diffusion,^{16–19} there have, somewhat remarkably, been very few studies of this surface using dynamic force microscopy (DFM, also known as non-contact atomic force microscopy (NC-AFM)).^{20,21}

Given not only the importance of the H:Si(100) surface as a substrate for next-generation device architectures^{18,22} but also the critical role that tip termination plays in DFM (particularly when light atom probes are used²³), we describe here the characteristic signatures of a hydrogen-terminated tip for both imaging and spectroscopy of the hydrogen-passivated Si(100) surface. Excellent agreement between the DFT calculations and experiment is found for tips which are hydrogen-terminated. We note that although Miura and Tsu-

kuda have previously carried out a theoretical analysis of the role of the tip termination on DFM imaging of H:Si(100),²⁴ with which our theoretical results are in broad agreement (see below), our work goes further by providing a direct comparison between experimental and theoretical *difference* spectra which can be exploited to elucidate the termination of the apex of the tip.

We used arsenic-doped low resistivity (6 mΩ cm) Si(100) throughout our experiments. These were prepared in an ultrahigh vacuum (UHV) chamber with a base pressure of 2×10^{-10} mbars. A clean Si(100) 2×1 surface was first produced by flashing the sample at 1150 °C followed by gradual cooling from 900 °C (at a rate of $\sim 1^\circ$ per second). The passivation of the sample was performed using a Specs GmbH thermal gas cracker positioned approximately 10 cm from the sample. Hydrogen was introduced into the chamber via the gas cracker until a pressure of $1\text{--}5 \times 10^{-7}$ mbars was reached. The sample was exposed for 3 min. (i.e., a total exposure of 10–70 Langmuirs) while held at a temperature of $\sim 400^\circ\text{C}$. Note that all temperature measurements have a large error bar of $\sim \pm 30^\circ\text{C}$. The anneal was continued as the sample was moved from the preparation chamber to the SPM chamber.

Measurements were made on a Createc GmbH LT STM-AFM system with Nanonis control electronics and software. qPlus sensors with tungsten tips (resonant frequency in the 17–21 kHz range, $Q \sim 3000\text{--}9000$ at 77 K) were used for both the STM and the AFM experiments. Tips were electrochemically etched and then sharpened using a focused ion beam *ex situ*. The apex was subsequently prepared during STM imaging using voltage pulsing and controlled tip crashes. All DFM images were acquired with tips that produced high quality atomic resolution STM images. Images were analyzed using the WSxM programme available from Nanotec Electronica.²⁵

Importantly, we did not apply a bias voltage to the sample in order to null out the contact potential difference. It has been recently shown²⁶ that in addition to the instrumental cross-talk that can exist between the tunnel current and Δf channels, there are important physical effects which can

^{a)}Electronic mail: philip.moriarty@nottingham.ac.uk.

couple these signals; Weymouth *et al.*²⁶ coined the term “phantom force” to describe this coupling. The phantom force effect is likely to be particularly important on surfaces without a high density of surface states, such as H:Si(100), where a significant fraction of the applied bias can drop in the semiconductor. Therefore, all DFM images and spectra discussed in this paper were acquired with 0 bias applied to the sample and the tip held at virtual ground at the input to the preamplifier. The sample (and microscope) were held at 77 K throughout our experiments. All images presented here were acquired in constant frequency shift mode; we show only the topographic data (i.e., the variation in the height of the tip as it tracks constant Δf).

Lack of a non-interacting site on the H:Si(100) surface, comparable to the cornerhole feature of the Si(111)-(7 × 7) reconstruction, renders accurate removal of the background contribution of long-range electrostatic and van der Waals from $\Delta f(z)$ (or $F(z)$) spectra problematic at best. We instead use a simple difference spectrum approach which produces data which we compare to simulated difference spectra generated via density functional theory (DFT). The Sader-Jarvis²⁷ method was subsequently used to extract forces from the frequency shift data. *Ab initio* DFT simulations were carried out using the SIESTA code²⁸ using a double-zeta polarized basis set in the generalized gradient approximation (GGA) with a Perdew-Burke-Ernzerhof density functional, norm-conserving pseudopotentials and a single $|\mathbf{k}| = 0$ point. The atomic structure was considered relaxed when forces on atoms fell below 0.01 eV/Å. This corresponds to a maximum change in the (x,y,z) coordinates of the atoms of (17.7, 61,

and 18 fm) in the last iteration before cut-off (for an extensive description please see Refs. 26–28). Local or long-range van der Waals interactions were not considered in our DFT calculations.

Fig. 1(a) is an STM image of the H:Si(100)-(2 × 1) (monohydride) surface (taken with a qPlus sensor) typically produced by the preparation conditions described above. A DFM image of the same H:Si(100) surface (although not the same surface region) is shown in Fig. 1(b). The atoms of the dimers image as depressions, rather than as protrusions (i.e., we see so-called “inverted” contrast), because the frequency shift above the H atoms is less negative (at a given height from the surface) than on the surrounding area, as shown by Miura and Tsukada.²⁴ In our experience, inverted contrast is observed *much* more frequently than “non-inverted” DFM imaging. Indeed, it is very difficult to coerce the tip apex into a state where it images the H atoms of the Si dimers as protrusions, rather than depressions. There is also a clear variation in contrast across the H:Si(100) surface with some dimers appearing much darker or much brighter than others (one possible origin of this variation is electrostatic interactions arising from local band bending due to adsorbates, defects, and/or sub-surface dopants. However, further, more systematic investigations are required in order to elucidate the physicochemical mechanisms underpinning this effect).

During our STM tip preparation procedure it is likely that the tip becomes terminated with a silicon or a hydrogen-passivated silicon cluster. To determine which of these options gives rise to inverted contrast and to provide detailed quantitative insights into the interaction forces between the

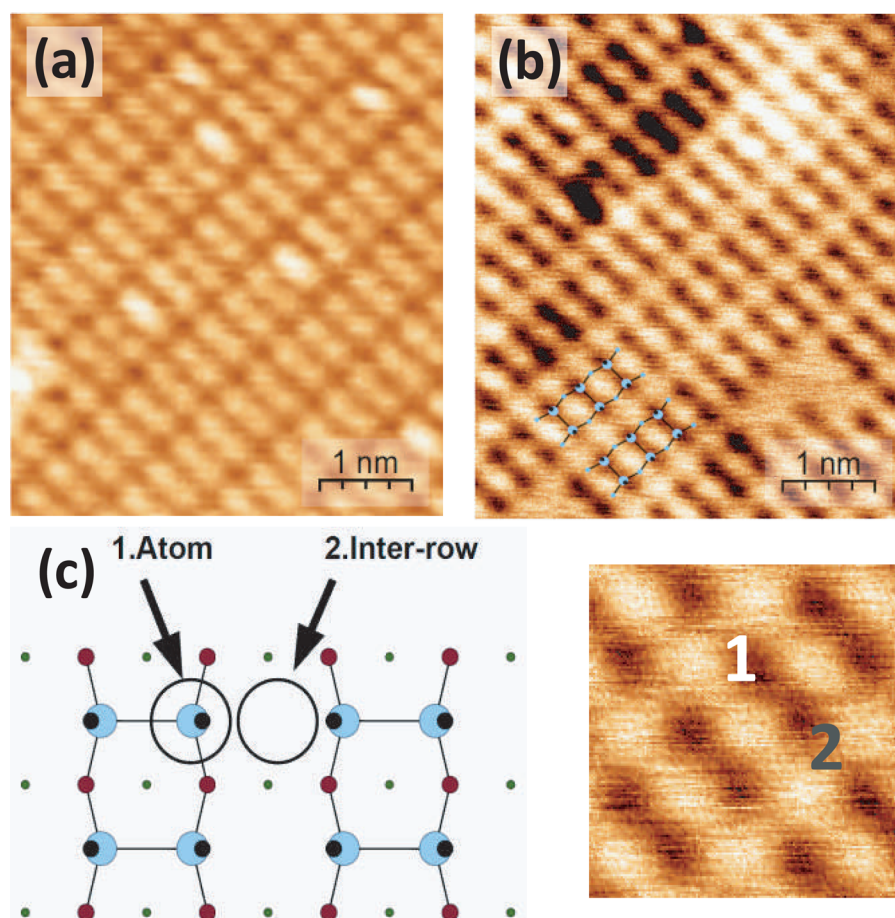


FIG. 1. (a) STM image of the H:Si(100)-(2 × 1) surface taken with a bias voltage of +1.5 V and set-point tunnel current of 100 pA; (b) constant frequency shift DFM image of the same surface (but a different region) where the H atoms of the dimers appear as depressions, i.e., “inverted” contrast ($\Delta f_p = -21.5$ Hz; oscillation amplitude = 300 pm). A ball-and-stick model showing the positions of the H-terminated dimers is overlaid on the image; (c) ball-and-stick model of the monohydride termination of the H:Si(100) surface which shows schematically the types of atomic site at which spectra were taken. The site numbers are overlaid on the accompanying DFM image for clarity.

DFM tip and the H:Si(100) surface, we have performed $\Delta f(z)$ spectroscopy at the two types of site shown in Fig. 1(c), namely, above an H atom (site 1) and between dimer rows (site 2). In principle, if a “null site,” i.e., an atomic site at the surface not associated with a short-range force (such as the Si(111)-(7 × 7) cornerholes), was available, then absolute, as opposed to relative, interaction potentials and tip-sample forces could be determined. However, we find that both types of site highlighted in Fig. 1(c) are associated with a short-range interaction.

We therefore adopted a difference spectrum approach to isolate the site-to-site variations in short range chemical force. Subtraction of spectra taken at different sites removes the long-range and therefore site-independent, electrostatic, and van der Waals forces. At the inter dimer-row sites (those labelled as 2 in Fig. 1(c)), the tip apex is furthest from the hydrogen atoms. These positions thus minimise the probe-sample interaction and were used to record “background” spectra which were subtracted from $\Delta f(z)$ measurements taken at the hydrogen atom positions. Multiple approach and retract spectra were taken at different sites and then averaged to produce $\Delta f(z)$ spectra which were subsequently converted to $F(z)$ curves.²⁷ From the scatter in these *difference* curves we estimate an error bar of ± 100 pN. This experimental uncertainty is particularly relevant for the discussion below.

Figs. 2(a) and 2(b) are the comparisons of experimental and theoretical difference spectra. In Fig. 2(a) the theoretical spectra have been calculated using a Si cluster terminated by an atom bonded in the “H3” configuration,²⁹ resulting in a single dangling bond at the apex. The DFT spectra in Fig. 2(b) were instead calculated using an “H3” tip terminated by a hydrogen atom (see inset to each figure). In both Fig. 2(a) and Fig. 2(b) we have plotted the experimental difference spectrum resulting from a subtraction of the inter-row spectrum from the above-H-atom spectrum (the corresponding above-H-atom and inter-row DFT spectra are also shown in Figs. 2(a) and 2(b), labelled as “atom” and “gap” in each case).

For the simulation with the unpassivated tip (Fig. 2(a)), there is a clear attractive interaction between the dangling bond of the H3 probe and the underlying H-passivated Si(100) surface, giving rise to a peak force of ~ 500 pN. This is in good agreement with the calculations of Masago *et al.*³⁰ In the gap between the dimer rows there is also a relatively strong interaction, but this peaks at a smaller tip-sample separation. When the “between dimer rows” curve is subtracted

from the “above-H-atom” data, a shallow “well” results with a maximum force difference of ~ 200 pN. Critically, the difference curve (filled green circles in Fig. 2(a)) is negative over a range of ~ 1 Å with a magnitude which is greater than our experimental error bar. The experimental data do not exhibit a similar attractive “dip.”

Figure 2(b) compares the same experimental force difference curve with DFT simulations for a H3 tip whose single dangling bond has been passivated by a hydrogen atom. In this case, there is only a very small attractive interaction (peaking at ~ 50 pN) between the passivated tip and the H:Si(100) surface. Between the rows the interaction is even weaker. The simulated difference spectrum is effectively flat (~ 0 pN) up to the point where it becomes positive-valued. Unlike the case of the unpassivated tip, we do not observe an attractive interaction in the simulated difference curve. Not only does this reproduce the lack of attractive component in the experimental difference curve, but the curvature of the simulated and experimental spectra match very well. The lack of a strong attractive component in the tip-sample interaction for the passivated tip underpins our frequent observation of inverted contrast in DFM imaging of H:Si(100); as for the experiments of Gross *et al.*,² with a CO-functionalized tip, the hydrogen termination stabilizes the tip, facilitating imaging in or close to the Pauli exclusion regime of the potential.

Although inverted contrast of the type shown in Fig. 1(b) is, as noted above (and in our experience), almost always observed when scanning H:Si(100), spontaneous tip changes can occur which reverse the contrast so that the H atoms appear as maxima rather than minima. We show three examples of this type of “non-inverted” contrast in Fig. 3. As for the clean Si(100)-c(4 × 2) surface,³¹ we observe a broad range of different image types depending on the tip state. While in Figs. 3(a) and 3(b) only the dimers are observed, in Fig. 3(c) each hydrogen atom is resolved. Spectroscopic measurements using a “non-inverting” probe have unfortunately not been possible to date because instabilities during imaging/spectroscopy reverted the tip apex to an “inverting” state.

In summary, we have determined the imaging and spectroscopic signatures associated with a H-terminated tip on the H:Si(100) surface. The difference spectrum approach, combined with DFT calculations, provides a protocol which can be used to identify H-passivated tips on silicon surfaces. This is of importance not only to elucidate and exploit the

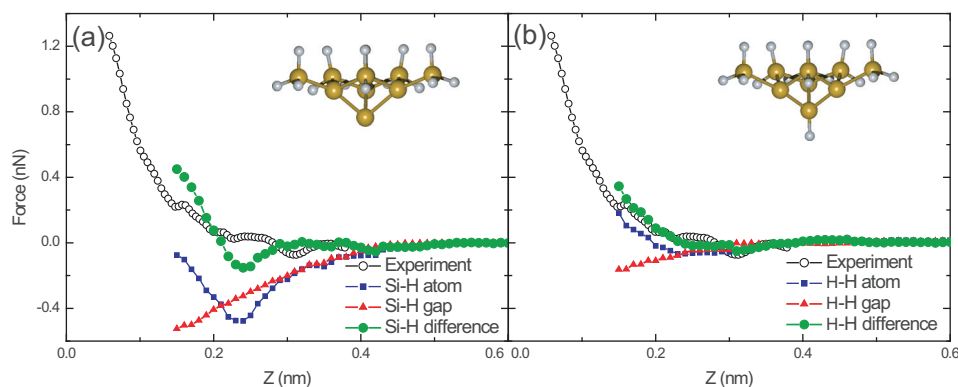


FIG. 2. Comparison of experimental and theoretical *difference* force-distance ($F(z)$) curves (see text) taken with (a) a reactive tip with a free Si dangling bond at its apex, and (b) a H-passivated tip. Open circles: experimental difference curve (Site 1-Site 2, see Fig. 1(c)); filled circles: DFT-simulated difference curve; filled squares: DFT spectra calculated above a hydrogen atom (Site 1); filled triangles: DFT spectra calculated at positions between the dimer rows (Site 2). Note that the same experimental difference curve is shown in (a) and (b) to facilitate direct comparison with theory.

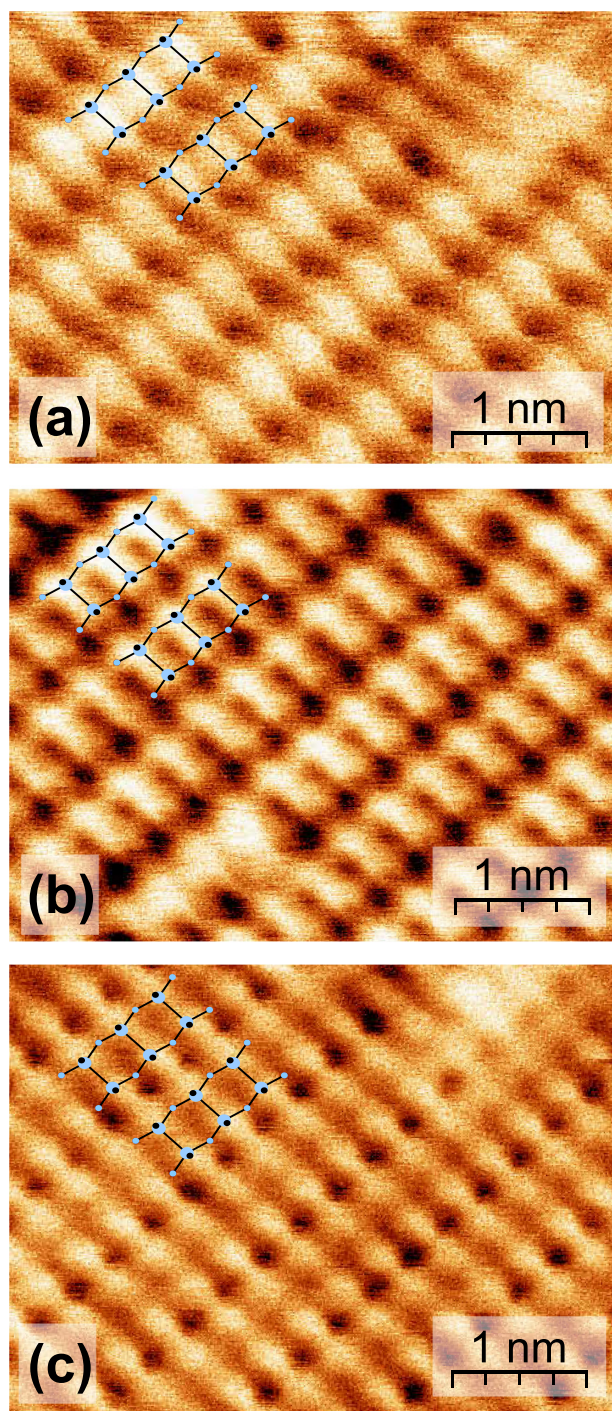


FIG. 3. DFM images taken with a non-inverting tip state. Dimers now appear as protrusions (a), (b), and at higher resolution (c), the individual H atoms are resolved (again, as protrusions). Images (a)-(c) acquired with $\Delta f_{sp} = -27.1$ Hz, -23 Hz, and -30 Hz, respectively; oscillation amplitude = 300 pm for all images. A ball-and-stick model showing the relationship between the DFM features and the passivated dimers of the H:Si(100) surface is overlaid on each image.

mechanisms underpinning DFM imaging^{2,5} but is of particular significance when it comes to atomic manipulation where the correct selection of tip state can be essential to drive a particular process such as atom extraction, deposition, or exchange.^{9,32}

P.J.M. thanks the Engineering and Physical Sciences Research Council (EPSRC) for the award of a fellowship (EP/G007837/1). S.J. also thanks EPSRC for a Ph.D. studentship. We also acknowledge funding from the European Commission's ICT-FET programme via the *Atomic Scale and Single Molecule Logic gate Technologies* (AtMol) project, Contract No. 270028, support from the Leverhulme Trust through grant F00-114/BI, and the support of the University of Nottingham High Performance Computing Facility.

¹F. Giessibl, S. Hembacher, H. Bielefeldt, and J. Mannhart, *Science* **289**, 422 (2000).

²L. Gross, F. Mohn, N. Moll, P. Liljeroth, and G. Meyer, *Science* **325**, 1110 (2009).

³L. Gross, N. Moll, F. Mohn, A. Curioni, G. Meyer, F. Hanke, and M. Persson, *Phys. Rev. Lett.* **107**, 086101 (2011).

⁴L. Gross, F. Mohn, N. Moll, G. Meyer, R. Ebel, W. Abdel-Mageed, and M. Jaspars, *Nat. Chem.* **2**, 821 (2011).

⁵R. Temirov, S. Soubatch, O. Neucheva, A. Lassise, and F. Tautz, *New J. Phys.* **10**, 053012 (2008).

⁶C. Weiss, C. Wagner, C. Kleimann, M. Rohlfing, F. Tautz, and R. Temirov, *Phys. Rev. Lett.* **105**, 086103 (2010).

⁷G. Kichin, C. Weiss, C. Wagner, F. Tautz, and R. Temirov, *J. Am. Chem. Soc.* **133**, 16847 (2011).

⁸Y. Sugimoto, P. Jelinek, P. Pou, M. Abe, S. Morita, R. Perez, and O. Custance, *Phys. Rev. Lett.* **98**, 106104 (2007).

⁹Y. Sugimoto, P. Pou, O. Custance, P. Jelinek, M. Abe, R. Perez, and S. Morita, *Science* **322**, 413417 (2008).

¹⁰S. Loth, S. Baumann, C. Lutz, D. Eigler, and A. Heinrich, *Science* **335**, 196 (2012).

¹¹Z. Sun, M. Boneschanscher, I. Swart, D. Vanmaekelbergh, and P. Liljeroth, *Phys. Rev. Lett.* **106**, 046104 (2011).

¹²G. Schull, Y. Dappe, C. González, H. Hulou, and R. Berndt, *Nano. Lett.* **11**, 3142 (2011).

¹³J. Boland, *Phys. Rev. Lett.* **65**, 3325 (1990).

¹⁴J. Boland, *Adv. Phys.* **42**, 129 (1993).

¹⁵M. Dürr and U. Höfer, *Surf. Sci. Rep.* **61**, 465 (2006).

¹⁶T. Shen, C. Wang, G. Abeln, J. Tucker, J. Lyding, P. Avouris, and R. Walkup, *Science* **268**, 1590 (1995).

¹⁷F. Ruess, L. Oberbeck, M. Simmons, K. Goh, A. Hamilton, T. Hallam, S. Schofield, N. Curson, and R. Clark, *Nano Lett.* **4**, 1969 (2004).

¹⁸B. Weber, S. Mahapatra, H. Ryu, S. Lee, A. Fuhrer, T. Reusch, D. Thompson, W. Lee, G. Klimeck, L. Hollenberg, and M. Simmons, *Science* **335**, 64 (2012).

¹⁹A. Bellec, D. Riedel, G. Dujardin, O. Boudiroua, L. Chaput, L. Stauffer, and P. Sonnet, *Phys. Rev. Lett.* **105**, 048302 (2010).

²⁰S. Morita and Y. Sugawara, *Jpn. J. Appl. Phys.* **41**, 4857 (2002).

²¹S. Araragi, A. Yoshimoto, N. Nakata, Y. Sugawara, and S. Morita, *Appl. Surf. Sci.* **188**, 272 (2002).

²²F. Ample, I. Duchemin, M. Hliwa, and C. Joachim, *J. Phys. Condens. Matter* **23**, 125303 (2011).

²³S. Hembacher, F. Giessibl, and J. Mannhart, *Science* **305**, 380 (2004).

²⁴N. Miura and M. Tsukada, *Jpn. J. Appl. Phys.* **41**, 306 (2002).

²⁵I. Horcas, R. Fernández, J. Gómez-Rodríguez, J. Colchero, J. Gómez-Herrero, and A. Baro, *Rev. Sci. Instrum.* **78**, 013705 (2007).

²⁶A. Weymouth, T. Wutscher, J. Welker, T. Hofmann, and F. Giessibl, *Phys. Rev. Lett.* **106**, 226801 (2011).

²⁷J. Sader and S. Jarvis, *Appl. Phys. Lett.* **84**, 1801 (2004).

²⁸J. M. Soler, E. Artacho, J. D. Gale, A. Garcia, J. Junquera, P. Ordejón, and D. Sanchez-Portal, *J. Phys. Condens. Matter* **14**, 27452779 (2002).

²⁹A. Sweetman, S. Jarvis, R. Danza, J. Bamidele, S. Gangopadhyay, G. Shaw, L. Kantorovich, and P. Moriarty, *Phys. Rev. Lett.* **106**, 136101 (2011).

³⁰A. Masago, S. Watanabe, K. Tagami, and M. Tsukada, *Jpn. J. Appl. Phys.* **48**, 025506 (2009).

³¹A. Sweetman, S. Jarvis, R. Danza, and P. Moriarty, *Beilstein J. Nanotechnol.* **3**, 25 (2012).

³²S. Jarvis, A. Sweetman, J. Bamidele, L. Kantorovich, and P. Moriarty "Role of orbital overlap in atomic manipulation," *Phys. Rev. B* (to be published).